

Investigating Cross-Sectional Size Distribution of Randomly Distributed 3D Spheres

Sai Pandian, ID: 29899923

Abstract—In this paper we present a 3-dimensional numerical simulation demonstrating that it is possible to reproduce the known planar cross-section distributions for Wicksell’s Corpuscule Problem, thereby recovering 3D particle size distributions from 2D cross-sections. We investigate the effects of different particle sizes on the experimental data, and show this method is accurate for 2 different starting 3D size distributions. We also present our findings on how sensitive this method is to experimental data and discuss its efficacy in a real world application such as identifying a material using a planar cross-section image from a microscope.

I. INTRODUCTION

IN the world of Material Science and Crystallography, it is often the case that a material is identified and classified using the distribution of its constituent particle sizes. However, direct observation of the particles so as to construct a distribution is often impossible. Using a modern microscope or laser imaging techniques, it is possible to observe particles in a cross-section of material. But the observed radii of particles in this cross-section do not necessarily correspond directly to the radii of the particles in the material, since the plane of the cross-section is not necessarily oriented such that the observed particles lie exactly on the plane. Thus, it becomes difficult to relate the observed distribution of particle sizes in the plane to the real distribution of particle sizes in the material.

Mathematically, determining the distribution of spherical particles from planar sections is a well known problem called Wicksell’s Corpuscule Problem [1], named after S. D. Wicksell, who solved the problem in 1925. With this solution, it is possible to determine the original distribution of spherical particles. Thus, it is possible to determine the distribution of particle sizes in a solid from its observed cross-section, allowing us to identify and classify materials better [2].

In this paper we aim to show that it is possible to reproduce theoretical results on cross-sectional distributions using numerical simulation, and it is thus possible to solve Wicksell’s Corpuscule Problem in this manner.

II. METHOD

Consider many spheres of different radii distributed randomly in space. For the purposes of the numerical simulation, we will consider a cube of length 20. The spheres were not allowed to overlap, which we ensured by placing the spheres such that if one sphere has vector position \vec{a} and radius r_1 and the other has vector position \vec{b} and radius r_2 , the spheres must have positions such that:

$$|\vec{a} - \vec{b}| > (r_1 + r_2)$$

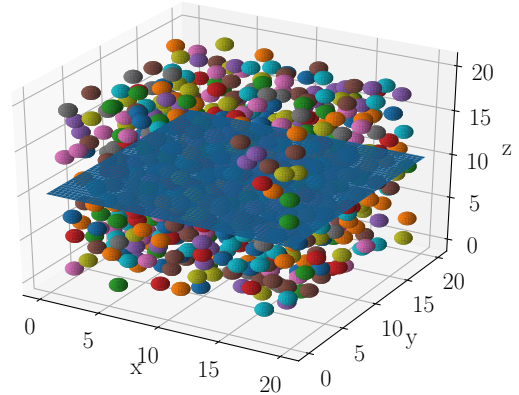


Fig. 1: 750 spheres of radius 0.7 distributed randomly in a cube of length 20, such that no sphere is touching or overlapping another sphere. A randomly oriented plane passes through the box and “cuts” through the spheres.

Random coordinates for a sphere are drawn from a uniform distribution and checked against every existing sphere until a set of coordinates is drawn that ensures no overlap, at which point the sphere is placed in space and the process is repeated until all the necessary spheres have been placed.

We then placed a plane into the cube, with a random orientation. The plane will “cut” through many of the spheres in the cube. This is shown in Figure 1. Here we see 750 spheres, each with radius 0.7 distributed randomly in a cube of length 20. The plane is shown in blue, and can be seen intersecting many of the spheres in the cube.

In order to obtain the planar cross-section, we employed the spherical cap method [3]. If we consider a sphere with centre $\vec{c}_0 = (x_0, y_0, z_0)$ and radius R , and a plane with equation $Ax + By + Cz = D$ such that $\vec{n} = (A, B, C)$ is the normal vector to the plane, then the distance from the centre of the circle to the closest point on the plane p_0 is given by ρ :

$$\rho = \frac{(\vec{c}_0 - \vec{p}_0) \cdot \vec{n}}{|\vec{n}|} = \frac{Ax_0 + By_0 + Cz_0 - D}{\sqrt{A^2 + B^2 + C^2}}$$

If $|\rho| < R$, then there is an intersection of the plane and the sphere. The radius of the circle r in the planar cross-section is given by:

$$r = \sqrt{R^2 - \rho^2}$$

And we then binned this radius to produce a histogram of the distribution of planar circle radii. It is also possible to recover

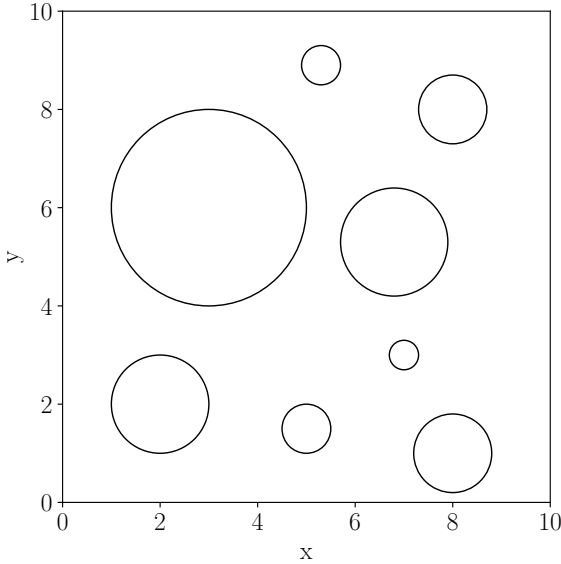


Fig. 2: Planar cross-section constructed using mock data. Spheres cut by the plane appear as circles on the plane, with radius dependent on the relative position of the spheres to the plane. This distribution of circles can be modelled.

the centre \vec{c} of the circle visible on the plane using:

$$\vec{c} = \vec{c}_0 + \rho \frac{\vec{n}}{|\vec{n}|} = (x_0, y_0, z_0) + \rho \frac{(A, B, C)}{\sqrt{A^2 + B^2 + C^2}}$$

Figure 2 presents a planar cross-section generated using this method and mock data. As we see, there are a range of circular radii observed since even though the spheres all had the same radius, they were at different distances from the plane, and were thus cut at different points. The many observed circular radii are binned to produce a distribution.

If $f(R)dR$ is the number of spheres per unit volume with radii in interval $[R, R+dR]$, then we can define a distribution $\phi(x)dx$ which represents the number of circles per unit area on the plane with radii in interval $[x, x+dx]$ [4]. This distribution is given by:

$$\phi(x) = \int_x^\infty \frac{xf(R)}{\sqrt{R^2 - x^2}} \quad (1)$$

We can compute this integral to obtain a theoretical planar distribution for different starting spherical radius distributions.

We first considered the case in which all the spheres had the same radius R_0 . In this case, the spherical radius distribution is simply a Dirac delta function centred on the radius R_0 .

If we compute the integral in Equation 1, replacing $f(R)$ with $\delta(R - R_0)$ we find:

$$\phi(x) = \int_x^\infty \frac{x\delta(R - R_0)}{\sqrt{R^2 - x^2}} = \frac{xH(R_0 - x)}{\sqrt{R_0^2 - x^2}} \quad (2)$$

where $H(R_0 - x)$ is the Heaviside function, which “turns on” the distribution only for $x < R_0$ as it is not possible to have a circular radius x larger than the spherical radius. So we aim to see our experimental data reproduce this distribution [5].

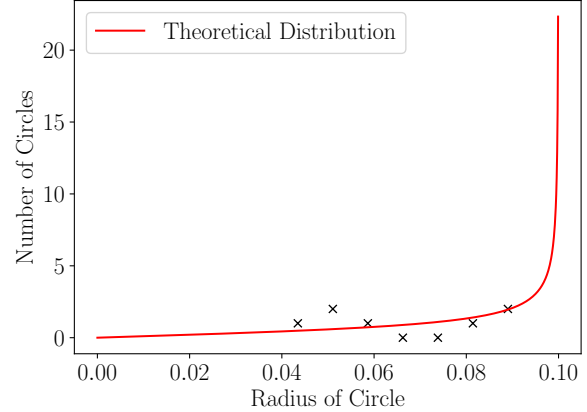


Fig. 3: Distribution of circle radii on plane for 750 spheres of radius 0.1 each. There are relatively few points since the spheres are small, so there is relatively small chance that they will be cut by the plane. So only a few circles are visible on the plane. The theoretical distribution is shown, with the experimental data matching this distribution, showing a slow increase in number of circles as radius increases.

We also investigated how changing the value of R_0 affects the experimental distribution.

We next considered the case in which each sphere has a radius R uniformly distributed in a range $R_1 < R < R_2$. In this case, we modify $f(R)$ in Equation 1 to be:

$$f(R) = \begin{cases} 1, & \text{if } R_1 < R < R_2 \\ 0, & \text{Otherwise} \end{cases}$$

In this case the integral in Equation 1 does not need to be computed with the limits shown, but instead with limits between R_1 and R_2 since $f(R)$ is 0 otherwise:

$$\begin{aligned} \phi(x) &= \int_{R_1}^{R_2} \frac{xf(R)}{\sqrt{R^2 - x^2}} \\ &= x \ln \left(\sqrt{R_2^2 - x^2} + R_2 \right) - x \ln \left(\sqrt{R_1^2 - x^2} + R_1 \right) \end{aligned} \quad (3)$$

Since this distribution produces complex numbers for $x < R_1$, we only consider the real part of this distribution, which appears to produce a peak at $x = R_1$.

III. RESULTS AND DISCUSSION

We found that for both the case of the spheres of constant radius, and the case of the spheres of varying radius, the experimental data reproduced a distribution in the same shape as the theoretical distribution.

We first investigated the case where we placed 750 spheres of radius 0.1 each in a cube of length 20. In this case we found that a plane in a random orientation intersects very few spheres, since the spheres are very small. The planar distribution is presented in Figure 3.

We observe relatively few experimental data points, as there were relatively few intersections with the plane. This was

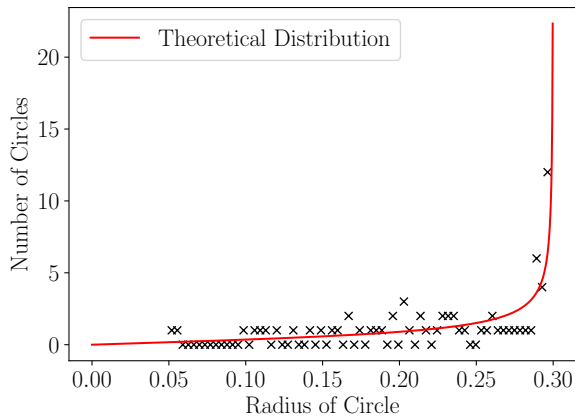


Fig. 4: Distribution of circle radii on plane for 750 spheres of radius 0.3 each. Compared to Figure 3, there are many more experimental data points, since it is more likely that the plane will intersect these larger spheres. The experimental data more clearly resembles the theoretical distribution, showing a strong increase in number of circles as radius increases towards the maximum of 0.3.

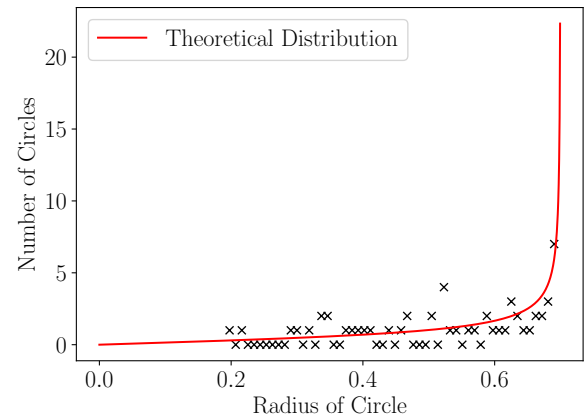


Fig. 5: Distribution of circle radii on plane for 750 spheres of radius 0.7 each. We do not observe much difference in how well the experimental data resembles the theoretical distribution between this figure and Figure 4. With larger sized spheres, the simulation becomes harder to run as it is more difficult to randomly place spheres in a finite space without overlap.

likely because the spheres' radii were very small compared to box length and there were relatively few spheres. While the theoretical distribution shows a strong increase near 0.1, this is not evident from the experimental data. We also see that there is a lot of variance between the points so the slow rise evident in the theoretical distribution is not clear in the experimental data. It is thus necessary that we have more spheres that intersect with the plane, in order to obtain a larger data-set.

We found that increasing the spheres' size or placing more spheres in the box, or making the box length smaller, are all good methods of increasing the number of intersections we observe, as they all increase the likelihood of intersection by increasing the ratio of sphere occupied space to total box space. We thus next used 750 spheres of radius 0.3 each. The planar cross-sectional distribution found is presented in Figure 4.

In Figure 4 we see that there are clearly more experimental data points. This is because more spheres had intersections with the plane. Compared to Figure 7b, the slow rise in the theoretical distribution is more closely followed by the experimental data. However, we still encounter significant variance and fluctuation in lower radius bins, even though the theoretical data is a smooth gradual increase. This is likely due to the relatively few number of circles populating these bins, causing greater relative difference between neighbouring bins. One method to solve this would be to use fewer bins, which would have the effect of "summing and averaging" neighbouring bins so the experimental data has a smoother trend. However, this would also reduce the number of data points so it was not implemented in our investigation.

The sharp rise in the theoretical distribution close to the maximum radius is also clear in the experimental data. It can

be understood intuitively that we expect to see more cross-sections with radius close to radius of the spheres since there is a greater probability of intersection with the centre of a sphere than any other point on the sphere.

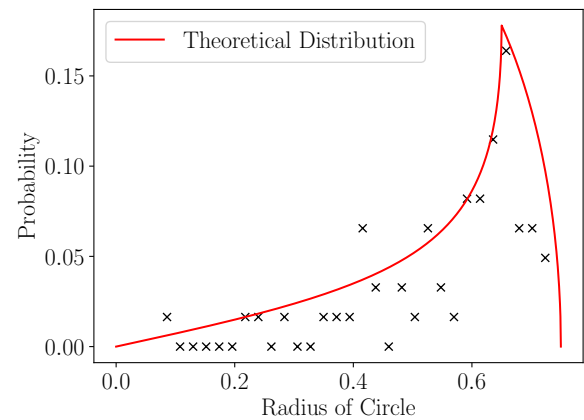


Fig. 6: Distribution of circle radii on plane for 750 spheres of radius R where $0.65 < R < 0.75$. The theoretical distribution is now different, although the experimental data still resembles this new distribution, showing a maximum around $R = 0.7$ and a sharp decrease after this. This is likely because there are more spheres with radii such that an overlap between 0 and 0.7 is possible, and relatively few spheres with radii such that a larger overlap is possible.

Increasing the size of the spheres further to a radius of 0.7, we might initially expect the experimental data to resemble the theoretical distribution even more closely, but this is not

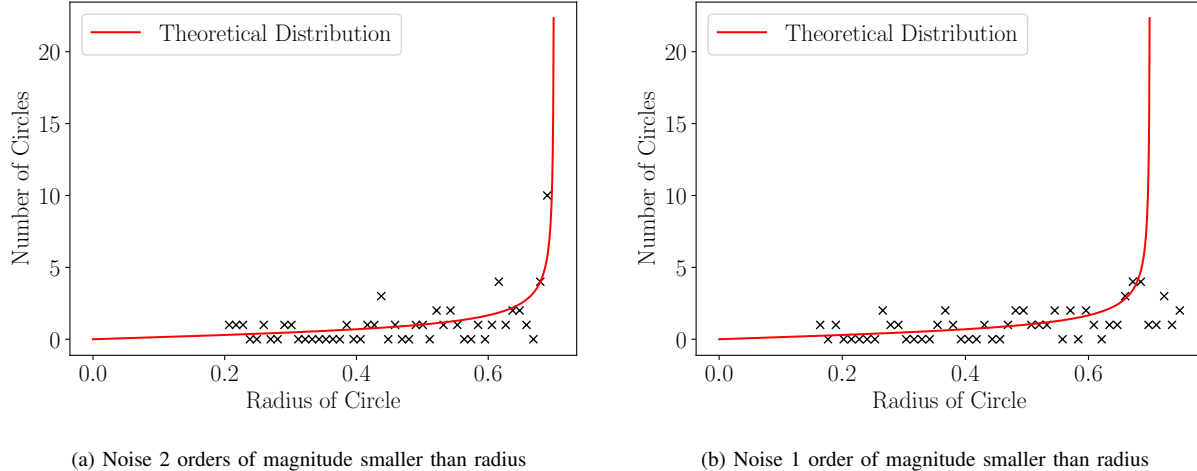


Fig. 7: Distribution of circle radii on plane for 750 spheres of radius 0.7 each. Each recorded radius has a random noise added to it in order to determine how sensitive the data is to experimental error. Figure 7a shows the distribution for an added noise 2 orders of magnitude smaller than the recorded radius, while Figure 7b is the same for noise 1 order of magnitude smaller. As we can see, the experimental data very resembles the theoretical distribution when noise of 2 orders of magnitude smaller are added. But this is not true when noise of 1 order of magnitude smaller is added, implying the data is very sensitive to experimental data.

what we see. Figure 5 presents the planar distribution for 750 spheres of radius 0.7 each.

In Figure 5, we see a similar experimental distribution to that of Figure 4, as opposed to a distribution that more closely resembles the theoretical distribution. While initially this may seem contrary to the notion that increasing size of spheres would increase the number of intersections and thus give a better distribution, this may simply be due to the fact that increasing the size of the spheres beyond a certain radius does not provide continually better results. We observe a similar number of intersections as the case with spheres of radius 0.3, and thus it is possible to conclude that the best experimental distribution is found for a spherical size that ensures a significant number of intersections. Though continually increasing spherical size provides diminishing returns.

Indeed, we found that making the sphere sizes much larger made the placing of the spheres in a finite space more difficult, and exponentially increased the time complexity of the placing algorithm. This is because if the placed spheres are too large, while it is initially easy to place spheres, as more are placed, more coordinates must be randomly drawn before one is found for the next sphere to be placed into. It is also possible that the algorithm never finds a possible coordinate for later spheres. One possible solution to this may be to use a better placing algorithm. Choosing a tight packing algorithm [6] would maximise the number of spheres of a given radius that can be placed. However, this would likely result in a less than random distribution of spheres if the spheres are all of identical sizes. This would likely cause some systematic error in the data, and so it was not investigated here. If we randomised the sizes of the spheres as we do in the next part of the investigation, the problem becomes significantly more complicated. Tight packing algorithms for irregular shaped objects are very

difficult to create and computationally expensive [7].

We next randomised the radius of each sphere to be in the range $0.65 < R < 0.75$. The experimental data for this simulation is presented in Figure 6.

Figure 6 presents the experimental data for 750 spheres with each sphere having a radius $0.65 < R < 0.75$. As we can see, the theoretical distribution has a very different shape to the case of constant sphere radius. We see that the theoretical distribution has a sharp peak centred around (but not precisely at) 0.65, the lower limit of the uniform range the radii were drawn from, and a sharp decrease after this point. This is likely due to the higher number of spheres available in the box which could be intersected so as to show a planar cross-section with radius ≈ 0.65 . In a range of radii between $0.65 < R < 0.75$, all the spheres in the box can be intersected so as to produce a circle of radius 0.65, but there will be fewer spheres which can be intersected to produce a circle of radius greater than this. So a peak at this point and then a sharp decrease is expected.

The experimental data resembles the theoretical distribution, clearly showing a peak and sharp decrease after. However, we also see that there is significant variance between bins, and there is a large scatter around the theoretical data. As explained for Figure 4, it would be possible to reduce this fluctuation by using fewer bins, at the cost of having fewer data points. With a more powerful computer, or if the simulation is optimised and written with a compiled language, there is also scope for significantly increasing the size and number of spheres used, which would provide better experimental data.

While there is significant fluctuation and scatter in all of the simulations presented so far, the shapes of the distributions were mostly clear, and they resembled the theoretical distribution. However, if the system is very sensitive to experimental error, it may be difficult to identify distribution shapes,

and thus prevent us from properly identifying the starting distribution of spherical radii. We therefore introduced some additional random error into the data. After the radii of the circles on the plane are calculated, a small random number is added to each radius. The random number is drawn from a uniform distribution in the range $[\frac{-r}{n}, \frac{r}{n}]$, where r is the circle's radius and n is the number of orders of magnitude we wish to choose the errors. We tested the system with errors 2 orders of magnitude smaller than the radii and 1 order of magnitude smaller than the radii. This is presented in Figure 7.

Figure 7a presents the distribution for 750 spheres of radius 0.7 each, with an added “noise” that is 2 orders of magnitude smaller than each measured radius. We can see that the experimental data looks very similar to the data presented in Figure 5. The shape of the distribution is also very clear and resembles the theoretical distribution.

Figure 7b presents the same simulation but with an added noise that is 1 order of magnitude smaller than each measured radius. Here we can see that the experimental data is unrecognisable, and the shape of the distribution is no longer clear. We thus conclude that the system is very sensitive to noise greater than 2 orders of magnitude compared to the measured data.

However, it would be more prudent to use a Gaussian distribution to draw the values of the noise. This is because it is likely that the many sources of error possible in an experimental measurement of particle cross-sections in a material will be convoluted together into a Gaussian distribution of errors due to the central limit theorem [8]. Thus, it would be necessary for any experimentalist attempting to carry out a similar investigation with real materials, perhaps to determine porosity [9], to carefully consider all errors in measurements.

IV. CONCLUSIONS

In this investigation we showed that it is possible to reproduce expected planar distributions for the Corpuscle Problem with a 3-dimensional numerical simulation of spheres distributed randomly in space, where a plane oriented randomly intersects the spheres. We investigated how effective this method of simulation is for different particle sizes, and showed that while initially larger particles provide better data since they allow for more intersections, continually increasing particle size becomes ineffective and computationally expensive.

We showed it was possible to reproduce the expected planar distributions for two starting spherical radii distributions: a Dirac delta distribution, in which all the spheres have the same radius, and a bounded uniform distribution, in which all the spheres' radii are drawn randomly from a uniform distribution. Both produce different shaped planar distributions but both provide data that resembles the theoretical distributions.

We also investigated how sensitive this method is to experimental error. We introduced some random noise into the system from a random uniform distribution and demonstrated that the system is very sensitive to noise greater than two orders of magnitude relative to measured data. Thus it is important for any experimentalist making measurements of particle cross-sections in a material to be very careful with

error handling, as any error larger than 2 orders of magnitude compared to measured data will result in great difficulty in reproducing the spherical radii distributions.

We therefore showed in this investigation that it is possible to use the known solutions to Wicksell's Corpuscle Problem to better identify and classify materials by using planar measurements to gain information about 3D particle distributions.

REFERENCES

- [1] B. S. D Wicksell, “THE CORPUSCLE PROBLEM. A MATHEMATICAL STUDY OF A BIOMETRIC PROBLEM,” Tech. Rep. [Online]. Available: <https://academic.oup.com/biomet/article-abstract/17/1-2/84/215917>.
- [2] J. N. Cuzzi and D. M. Olson, “Recovering 3D particle size distributions from 2D sections,” Tech. Rep., 2016. [Online]. Available: <https://ntrs.nasa.gov/search.jsp?R=20170001990>.
- [3] M. Sykes and C. Comstock, *Solid Geometry*. Rand McNally, 1922, 81 ff. [Online]. Available: <https://archive.org/details/solidgeometry01comsgoog>.
- [4] M. Kiderlen, “Old and New on Wicksell's Corpuscle Problem Motivation: Fundamental formula of stereology,” Tech. Rep., 2011.
- [5] M. Kong, R. N. Bhattacharya, C. James, and A. Basu, “A statistical approach to estimate the 3D size distribution of spheres from 2D size distributions,” *Bulletin of the Geological Society of America*, vol. 117, no. 1-2, pp. 244–249, Jan. 2005, ISSN: 00167606. DOI: 10.1130/B25000.1.
- [6] D. Z. Chen, X. Hu Ý, Y. Huang, Y. Li, and J. Xu, “Algorithms for Congruent Sphere Packing and Applications,” Tech. Rep., 2001.
- [7] Y. Ma, Z. Chen, W. Hu, and W. Wang, “Packing Irregular Objects in 3D Space via Hybrid Optimization,” Tech. Rep. 5, 2018.
- [8] M. R. Islam, “Sample size and its role in Central Limit Theorem (CLT),” *International Journal of Physics & Mathematics*, vol. 1, no. 1, pp. 37–47, Jun. 2018. DOI: 10.31295/ijpm.v1n1.42.
- [9] S. N. Lekakh, V. Thapliyal, and K. Peaslee, “Use An Inverse Algorithm For 2D-3D Particle Size Conversion And Its Application To Non-Metallic Inclusion Analysis In Steel,” Tech. Rep.